

INHERENTLY ROBUST MICRO GYROSCOPE ACTUATED BY PARAMETRIC RESONANCE

Laura A. Oropeza-Ramos, Christopher B. Burgner, and Kimberly L. Turner
Mechanical Engineering Department, University of California, Santa Barbara

ABSTRACT

The sensitivity loss, commonly presented in micro gyroscopes based on harmonic oscillators [1], is overcome by using parametric resonance as an actuation mechanism. This operation has been analytically studied in IEEE-Sensors'05 [2] and preliminary dynamical characterization and experimental setup has been presented in IDETC/CIE-ASME'07 [3]. The device is fabricated using SOI process and in this paper we report complete rate table characterization including off-axis isolation, drift, hysteresis and noise of the micro gyroscope with an additional amplification stage.

1. INTRODUCTION

Gyroscopes are used in many commercial applications in which rotation measurements are needed, including hand held GPS, active suspension, and munitions guidance systems. In macroscopic systems, typical designs include rotating parts with bearings. In batch micro fabrication, due to geometry and process restrictions, often vibrating structures are used instead. Vibratory rate gyroscopes utilize the Coriolis force to transfer energy between modes of oscillation.

To achieve high sensitivity in conventional micro rate gyroscopes based on harmonic oscillators, the drive and the sense resonant frequencies are typically designed and tuned to match, and the device is controlled to operate at or near the peak of the response curve (where amplitude is defined by the Q -factor) [4]. However, current micro fabrication processes produce asymmetries causing frequency mismatching between modes, translating to drastic loss of sensitivity [1]. Although solutions to overcome frequency mismatching have been pursued [5]-[8], many of them involve adding complexity to the system by including additional controllers, additional degrees of freedom [9] or utilizing multiple drive mode oscillators [10].

A parametrically excited system is described by differential equations with time dependent coefficients and has been studied in micro oscillators [11]-[14], which show large amplification over a wide range of excitation frequencies. This response can be used to eliminate the frequency mismatching and preliminary results presented in [2] and [3] motivate further investigation into parametric resonance effects on important characteristic gyroscope parameters such as drift, off-axis rotation, hysteresis, and noise.

2. THE SYSTEM

The resonant Coriolis force sensor proposed is a two degree of freedom (DOF) structure (Figure 1) whose model and design have been detailed in [3]. The drive-mode (x -dir) actuator based on non-interdigitated comb-fingers generates

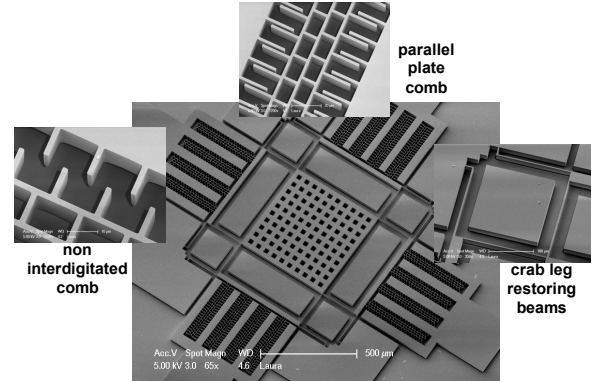


Figure 1. Micrograph of the micro gyroscope fabricated using a single mask SOI process on a 20 μ m Si layer over 5 μ m insulator, obtaining high aspect ratio structures that yield good off-axis isolation.

a force related to time and displacement dependent stiffness coefficients. The sense-mode (y -dir) is detected by a set of parallel plates. Constructing the device in this way, the micro gyroscope consists of 1-DOF driving oscillator governed by a nonlinear Mathieu equation [12], [15] and 1-DOF sensing oscillator governed by a Duffing model. Both of them are coupled by the Coriolis force as is modeled in the following normalized equations:

$$\begin{aligned} x'' + \alpha_x x' + (\delta_x + 2\beta_x \cos 2\tau)x + \\ + (\delta_{x3} + 2\beta_{x3} \cos 2\tau)x^3 - \gamma y' = 0 \\ y'' + \alpha_y y' + \delta_y y + \delta_{y3} y^3 + \gamma x' = 0 \end{aligned} \quad (1)$$

$\alpha_x = \frac{2c_x}{m\omega}$	$\alpha_y = \frac{2c_y}{m\omega}$
$\beta_x = \frac{2r_1 V_A^2}{m\omega^2}$	$\beta_{x3} = \frac{2r_3 V_A^2}{m\omega^2}$
$\delta_x = \frac{4(k_{x1} + r_1 V_A^2)}{m\omega^2}$	$\delta_{x3} = \frac{4(k_{x3} + r_3 V_A^2)}{m\omega^2}$
$\delta_y = \frac{4k_y}{m\omega^2}$	$\delta_{y3} = \frac{4k_{y3}}{m\omega^2}$
$\gamma = \frac{4\Omega_z}{\omega}$	$(\cdot)' = \frac{d(\cdot)}{d\tau}$

Table 1. Nondimensional parameters in equation (1).

The derivative operator and parameters are summarized in Table 1, where m is the mass, c_x and c_y are the damping coefficients, k_* and k_{*3} are the linear and the cubic stiffness coefficients, r_1 and r_3 are electrostatic coefficients that depend on the physical dimensions and spacing of the electrostatic comb-drives, V_A is the voltage amplitude applied across the drives, ω is the driving frequency, and Ω_z is the external angular velocity to be detected. Note that the expression for the primary mode (x -direction) in (1) is in the form of a nonlinear Mathieu equation, which is a second order nonlinear differential equation with periodic coefficients.

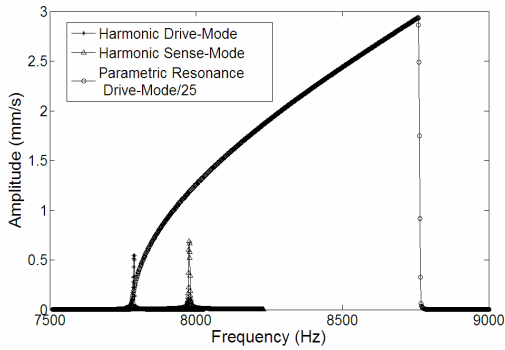


Figure 2. Experimental frequency response of the drive-mode (* harmonic, o parametric) and sense-mode (^ harmonic) tracked using laser vibrometry. Note the clear mismatching between drive and sense natural frequencies. Using a parametric resonance actuation (which amplitude is divided by 25 for scaling purposes) in the drive oscillation, the sense-mode can be induced by Coriolis coupling in the presence of structural parameter variations.

In contrast to a harmonic response where the excitation appears as an inhomogeneity in the governing differential equations, here the excitation appears as time-varying stiffness coefficients in the governing differential equations. In a harmonic oscillator a small excitation can produce a large response only when the driving frequency is close to the linear natural frequency and the amplitude depends on the damping coefficient (Q -factor). However, a small parametric excitation can produce a large response when the driving frequency is away from the natural frequency of the system and the amplitude does not depend on the viscous damping term to the first order.

Dynamic Characterization

Figure 2 gives experimental evidence, obtained through laser vibrometry [16], [17], that when the driving frequency is near twice the fundamental resonance of the drive-mode, a small parametric excitation can produce a large response over a few hundred Hz of frequencies. In this case, the mechanical and electrical nonlinearities dominate the parametric amplitude. Therefore the mismatch of the drive and sense fundamental frequencies still allows the sense-mode oscillations to be induced by Coriolis coupling.

The parametric regime of the drive-mode begins at a driving frequency of $f_a=2f_x=15,770$ Hz; nevertheless, this actuation generates a response that is below the natural frequency of the sense-mode $f_s=7,977$ Hz. Consequently, to achieve the highest sensitivity of the sense-mode, the actuation frequency simply needs to be changed to $f_a=2f_y=15,950$ Hz. This is possible due to the inherent flexibility of parametric excitation already discussed.

3. RATE TABLE PERFORMANCE

Figure 3 shows a pictorial diagram of the experimental set up implemented. All experiments were performed at $50mTorr$ pressure ($Q\sim 7000$) and the rate table sensor response was detected with a commercial CMOS capacitive readout wire bonded to the gyroscope on a chip.

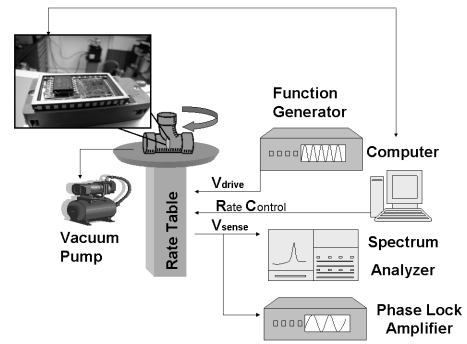


Figure 3. Schematic of the experimental set up.

Constant Angular Rate, Scale Factor and Linearity

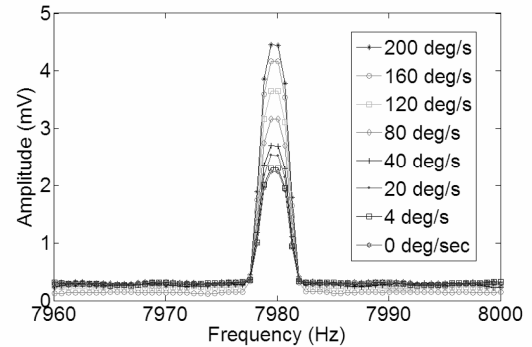


Figure 4. Spectrum of the sensor output induced by different constant angular velocities with an additional stage amplification of 2.

The spectrum of the sensor output, before demodulation, induced by different constant angular velocities is plotted in Figure 4. Note that even in the presence of error signals such as quadrature error, offsets, circuit noise, etc., the system is able to detect angular rate reliably. The resulting characteristics used to determine the scale factor and linearity of the output response of the gyroscope are shown in Figure 5. The gyroscope demonstrates a scale factor of $11 \mu V/deg/sec$ in a measurement range of $\pm 150 deg/sec$. The data presents a strong linearly correlation since the R^2 -nonlinearity is better than 0.8% .

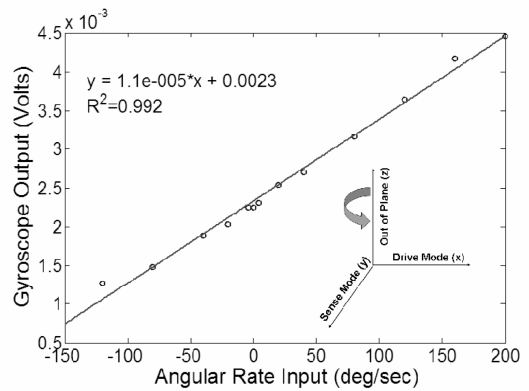
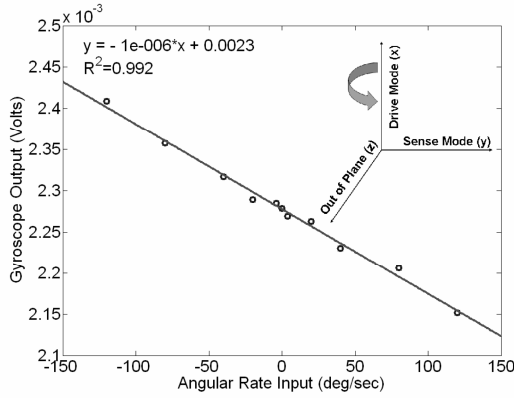
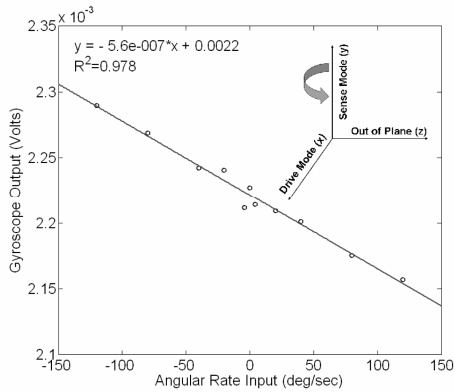


Figure 5. The measured gyroscope output in response to angular rate inputs between $\pm 150 deg/sec$ range.

Off-axis response



(a) Device tilted 90 deg with respect to y



(b) Device tilted 90 deg with respect to x

Figure 6. Response of the micro gyroscope to off-axis angular rotation testing.

Figures 6(a) and 6(b) show the output response when the gyroscope is tilted 90 deg with respect to y and x directions respectively. Comparing the curve slopes, it is determined that the device presents an off-axis isolation ratio between 11 and 20. This is in the range of expected values considering the SOI-based structure has an aspect ratio of 10.

Demodulation

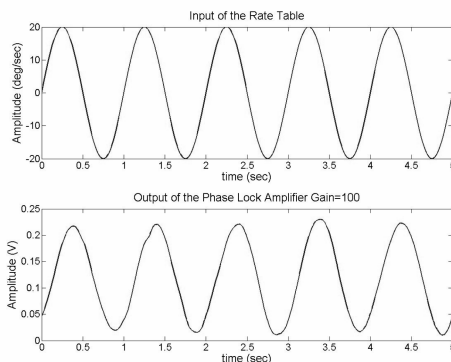


Figure 7. (top) 1 Hz sinusoidal signal input to the rate table. (bottom) Output of the Phase Locked Amplifier with a reference signal frequency of 7,977.19 Hz.

A Phase Lock Amplifier (PLA) was connected to the circuit output to demodulate the rate table signal detected by the micro gyroscope. A sinusoidal signal of amplitude 20 deg/sec and frequency of 1 Hz is applied to the rate table and a reference signal close to $f_s = 7,977$ Hz is provided to the PLA, which therefore tracks the signal variation at this frequency. Figure 7 shows the output of the PLA. Clearly, the micro gyrosopic system follows the rate table oscillation at 1 Hz.

Resolution and noise

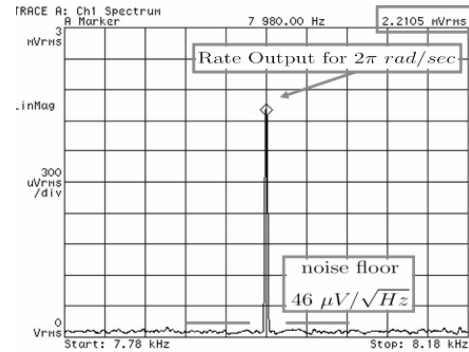


Figure 8. Sense-mode output detected with the spectrum analyzer in response to a 2π rad/sec rate input.

Figure 8 shows a screen shot of the Spectrum Analyzer which was used to monitor the output of the micro gyroscope. The peak amplitude is tracked and detected to be 2.2105 mV_{rms} for a rate input of 2π rad/sec, which gives a mechanical rate sensitivity of 352 μ V_{rms}/deg/sec. The noise floor is measured to be 46 μ V_{rms}/sqrt(Hz). The noise-equivalent rate of the gyroscope then corresponds to 0.1deg/sec/sqrt(Hz). Considering the scale factor of the system defined above, the measured rms noise floor is equivalent to fluctuations of 6 deg/sec.

Drift and Hysteresis

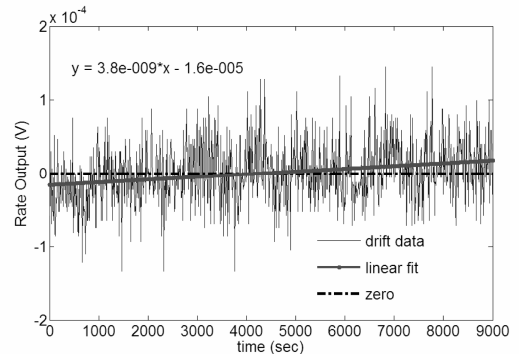


Figure 9. Stochastic variation of the MEMGyroscope ZRO bias measured during $t=2.5$ h. Note that the amplitude is divided by the PLA gain of 42.

For a period of 2.5 hours, the zero rate output (ZRO) signal was acquired through the PLA to analyze the signal drift, and the result divided by the PLA gain of 42 is plotted in Figure 9. The data is linearly fitted and from the slope of the

curve and considering the scale factor obtained above, the drift is calculated to be equivalent to 1.2 deg/sec/h . It is also important to note that the signal presents fluctuations that correspond to rate changes of 9 deg/sec . The difference between this value and the measured noise floor equivalent to 6 deg/sec is probably due to the phase-error in the PLA.

The data plotted in Figure 10 shows the transient response to a sequence of accumulative 20 deg/sec steps in a range of $\pm 100 \text{ deg/sec}$. The test started from zero-rate and ended at the same zero input stage. Observe that the performance of the micro gyroscope presents practically no hysteresis.

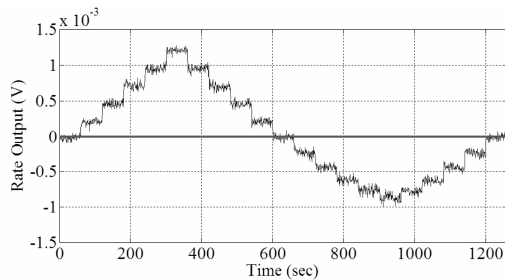


Figure 10. Stairs testing of the measured gyroscope output in response to angular rate inputs from zero-rate between $\pm 100 \text{ deg/sec}$ with 20 deg/sec steps and then back to zero-rate.

4. DISCUSSION AND CONCLUSIONS

The experimental array for rate table characterization is set up and a CMOS commercial capacitive readout through the sense-mode port is used to detect the induced Coriolis signal at 50 mTorr pressure. Our device has demonstrated a scale-factor of $11 \mu\text{V/deg/sec}$ and a nonlinearity of 0.8% both within $\pm 150 \text{ deg/sec}$ measurement range. The device presents an off-axis isolation ratio between 11-20 on y and x directions, which agrees well with the SOI-based structure of aspect ratio 10. Off-axis isolation can be improved using thicker SOI wafers. The noise-equivalent rate of the gyroscope corresponds to $0.1 \text{ deg/sec/sqrtHz}$, the drift is calculated to be equivalent to 1.2 deg/sec/h in 2.5 h and there is practically no evidence of hysteresis in the system.

This resonant Coriolis force sensor meets the rate grade specifications stated in [1]. For tactical grade applications, resolution must be improved. It can be enhanced by fine tuning the electronics, including the PLL process, the hybrid CMOS connection, and adding a Kalman filter. In conclusion, the unique properties of parametric resonance make this micro gyroscope robust to parameter variations over a wide spectrum and its performance has been fully characterized.

ACKNOWLEDGMENT

This work is supported by the Institute for Collaborative Biotechnologies at UCSB under grant DAAD19-03-D-0004.

REFERENCES

[1] N. Yazdi, F. Ayazi, and K. Najafi, "Micromachined inertial sensors", *Proc. of the IEEE*, vol. 86 No. 8,

August 1998.

- [2] L. Oropeza-Ramos and K. Turner, "Parametric amplification in a memgyroscope", *IEEE Sensors*, 2005.
- [3] L. Oropeza-Ramos, C. B. Burgner, C. Olroyd, and K. Turner, "Characterization of a novel memgyroscope actuated by parametric resonance", *IDETC/CIE*, Sept 2007.
- [4] W. Clark, "Micromachined vibratory rate gyroscopes", PhD Thesis, University of California, Berkeley, 1997.
- [5] S. Park and R. Horowitz, "Adaptive control for the conventional mode of operation of mems gyroscopes", *Journal of Microelectromechanical Systems*, vol. 12, pp. 101-108, Feb 2003.
- [6] R. Leland, "Adaptive mode tuning for vibrational gyroscopes", *IEEE Transactions on Control Systems Technology*, vol. 11, pp. 242-247, March 2003.
- [7] C. Painter and A. Shkel, "Active structural error suppression in mems vibratory rate integrating gyroscopes", *Sensors Journal, IEEE*, vol. 3, pp. 595-606, Oct 2003.
- [8] A. Shkel, R. Horowitz, A. Seshia, S. Park, and R. Howe, "Dynamics and control of micromachined gyroscopes", *Proc. of American Control Conference*, vol. 3, pp. 2119-2124, August 1999.
- [9] C. Acar and A. Shkel, "Nonresonant micromachined gyroscopes with structural mode-decoupling", *IEEE Sensors Journal*, vol. 3, No.4, August 2003.
- [10] —, "An approach for increasing drive-mode bandwidth of mems vibratory gyroscopes", *Journal of Microelectromechanical Systems*, vol. 14, June 2005.
- [11] R. Baskaran, "Parametric resonance and amplification in single and coupled micro electro mechanical systems", PhD Thesis, University of California, Santa Barbara, September 2003.
- [12] K. L. Turner, S. A. Miller, P. Hartwell, N. MacDonald, S. Strogatz, and S. Adams, "Five parametric resonances in a microelectromechanical system", *Nature*, pp. 149-152, 1998.
- [13] W. Zhang, "Nonlinear dynamics of micro-electro-mechanical oscillators and their application in mass sensing", PhD Thesis, University of California, Santa Barbara, August 2004.
- [14] B. DeMartini, J. F. Rhoads, K. L. Turner, S. W. Shaw, and J. Moehlis, "Linear and nonlinear tuning of parametrically excited mems oscillators", *Journal of Microelectromechanical Systems*, vol. 16(2), April 2007.
- [15] W. Zhang, R. Baskaran, and K. Turner, "Effect of cubic nonlinearity on auto-parametrically amplified resonant mems mass sensor", *Sensors and Actuators A (Physical)*, vol. 102, Issues 1-2, pp. 139-150, Dec 2002.
- [16] K. L. Turner, P. Hartwell, and N. MacDonald, "Multi-dimensional mems motion characterization using laser vibrometry", *Transducers*, pp. 1144-1147, 1999.
- [17] K. L. Turner, "Sensing picogram masses-laser vibrometry leads to breakthroughs in mems dynamic analysis", *Laser Measurement Systems, LM Info Special Magazine - Polytec*, vol. Issue 1, May 2005.